Pergamon

Cement and Concrete Research 30 (2000) 1941–1945

CEMENT AND CONCRETE RESEARCH

Analysis of iron oxides accumulating at the interface between aggregates and cement paste

Kalliopi K. Aligizaki[a,]*, Mario R. de Rooij[b], Digby D. Macdonald[a]

[a]*Center for Electrochemical Science and Technology, 201 Steidle Building, The Pennsylvania State University, University Park, PA 16802, USA*
[b]*Faculty of Civil Engineering, Delft University of Technology, Postbox 5048, 2600 GA Delft, Netherlands*

Received 17 February 2000; accepted 8 August 2000

Abstract

Iron oxides formed by the corrosion of a steel reinforcing bar were found to accumulate at interfaces between aggregate and cement paste in Portland cement-based concrete. Microstructural characterization of the zones of oxide was carried out using optical microscopy, scanning electron microscopy (SEM), and energy dispersive X-ray (EDX) spectroscopy. The study showed that the oxide layer has an average thickness of about 1.5 mm, and consists of inner and outer layers with different types of oxides in each layer. A mechanism based on the Schikorr reaction is proposed for the preferential formation of iron oxides in the two layers taking into account local variations in pH of the pore solution during the early ages of the cement paste. © 2001 Elsevier Science Ltd. All rights reserved.

Keywords: Corrosion; Backscattered electron imaging; EDX; Schikorr reaction; Interfacial transition zone

1. Introduction

Characterization of the interface between aggregate and bulk cement paste [commonly known as the interfacial transition zone (ITZ)] and its influence on the properties of cement-based materials has been the subject of study for many years as this zone is considered to be a "weak link" in the composite. It is generally accepted that in ordinary Portland cement concrete, the zone of cement paste near an aggregate interface is microstructurally different from the cement paste more distant from the interface. The ITZ is usually indicated as aureole extending on average 30–50 μm away from the aggregate, the estimate usually being based on the basis of microscopic observations [1]. Chemical and microstructural characteristics of the ITZ between paste and aggregate have been considered to influence the durability as well as the mechanical properties of concrete. Local variations in microstructure include differences in composition and greater porosity, with many interconnected pores and consequently, high permeability [2].

The transition zone between the steel reinforcing bar and cement paste has also been studied [3–5]. A lime-rich interfacial zone surrounds the steel embedded in cement-rich, dense concrete. Large $Ca(OH)_2$ crystals have been found at the interface between the steel and cement paste in the presence of chlorides.

The importance of the ITZ in transportation phenomena has been demonstrated in terms of an increased diffusivity [6,7] and accumulation of ions in the zone [8]. To the authors' knowledge, only one case has been reported in the technical literature of iron oxides accumulating at the interface between quartz aggregate and cement paste from a nearby corroding reinforcing steel bar [8]. That researcher did not report any differences in the identities of oxides formed in the ITZ. In other studies, corroded steel bars embedded in concrete formed different types of oxides around the steel bar [5,9].

This study concerns the microstructural characterization of the zone of accumulated iron oxides observed around aggregates in concrete from a nearby corroding steel bar using backscattered electron imaging and energy dispersive X-ray (EDX) spectroscopy. A mechanism for the formation and accumulation of different types of iron oxides is also proposed.

---

* Corresponding author. Tel.: +1-814-863-8378; fax: +1-814-863-4718.

E-mail address: aligizaki@alumni.psu.edu (K.K. Aligizaki).

0008-8846/00/$ – see front matter
PII: S0008-8846(00)00392-6

2. Experimental procedure

2.1. Source of specimens

The specimens used in this study are part of a greater project that involved the corrosion of a steel bar in concrete specimens [10]. The concrete mixtures produced were air-entrained and prepared with type I Portland cement, with a cement factor of 400 kg/m^3, and coarse and fine limestone aggregates. The mixtures contained 3.7% of NaCl by mass of cement, in order to accelerate corrosion of the steel bars. During the final stages of the study, after the specimens were cracked open in order to remove the steel bars and determine the degree of corrosion, it was noticed that iron oxides had accumulated around some aggregates (Fig. 1). Oxide accumulation around aggregates was observed on the concrete fracture surface in several specimens from different concrete mixtures. It was noticed that this accumulation of iron oxides occurred only around aggregates very close to the reinforcing steel bar and not at all in any other location. Pieces of concrete containing these areas were removed for further study. The structure and composition of the area surrounding the aggregates was studied using an optical microscope, backscattered electron imaging, and point energy dispersive spectroscopic analysis. All studies were performed on the fractured surfaces of concrete without additional preparation.

2.2. Optical microscopy observations

The optical microscope used in this work was a MZ6 from Leica with a color JVC digital camera. The magnification used was 6.4 ×. Examinations of the cement paste/aggregate interface by optical microscopy were carried out for all specimens where corrosion product accumulation at the interfaces was observed. In all cases, the same characteristics were found: a thin layer, black–dark brown in color, in immediate contact with the aggregate, noted in the following as the "internal oxide layer," and a thicker layer, brown–dark orange in color, close to the cement paste, which was identified below as the "external oxide layer" (Fig. 2). Corrosion products of the similar brown–dark orange color were observed to fill the pores of the cement paste up to an average distance of about 3 mm from the aggregate/cement paste interface.

2.3. Backscattered electron imaging

A Philips XL30 environmental scanning electron microscope (ESEM), equipped with secondary and backscattered electron detectors operating at an accelerating voltage of 20 keV, was used for backscattered electron imaging. A series of backscattered electron images were taken from neighboring areas and were mounted one next to the other to reproduce the surface of the aggregate, oxide layer, and surrounding cement paste. One of these surfaces is shown in Fig. 3.

The backscattered electron images show that the layer of iron oxides measured has an average thickness of 1100 μm (ranging from 900 to 1300 μm); more specifically, the internal oxide layer measured has an average thickness of 200 μm, while the external oxide layer has an average thickness of 900 μm.

Another observation worth noting is that even though microcracking in the cement paste surrounding the oxides was observed, it is considered to be insignificant. Since iron oxide formation is accompanied by an increase in volume, it should lead to microcracking in the surrounding cement paste. The absence of significant cracking in the

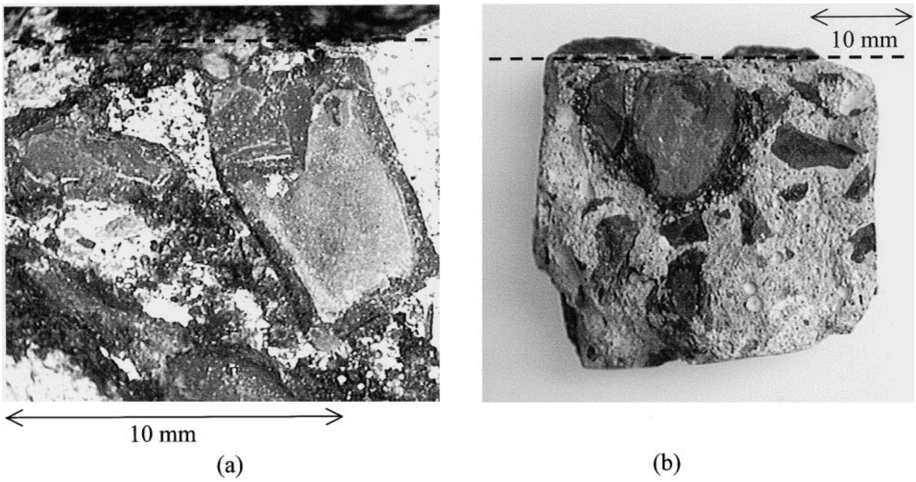

Fig. 1. Iron oxides accumulating around aggregates very close to a corroding reinforcing steel bar in air-entrained concrete containing chlorides in the initial mixture. The cement content was 400 kg/m^3, water-to-cement ratio = 0.45, 3.7% NaCl by mass of cement added in the initial mixture. The figures are from different specimens from the same mixture. The dotted lines indicate the position of the reinforcing steel bar.

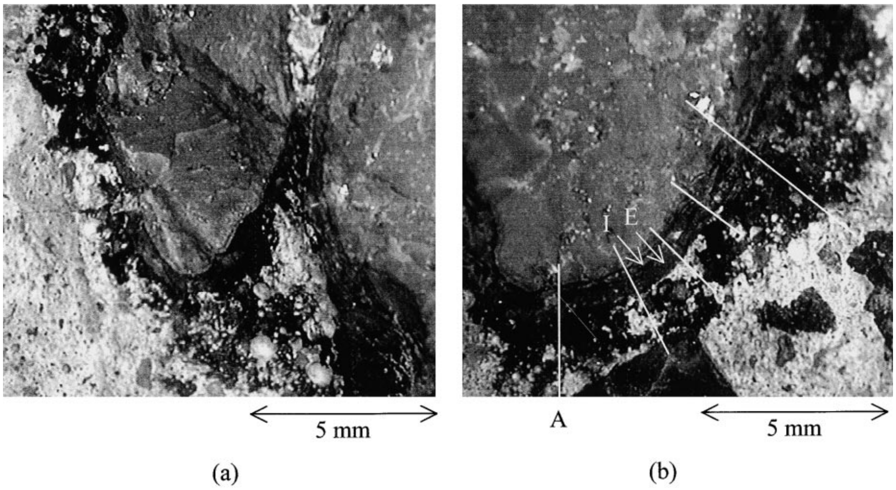

Fig. 2. Details of the iron oxides around the aggregates from the specimen shown in Fig. 1b. The lines indicate the positions along which the EDX element point analyses were conducted. In (b), I identifies the internal oxide layer, and E the external oxide layer.

cement paste around the aggregate and the iron oxide layer indicates that the accumulation of oxides and the related expansion occurred at early stages, when the paste was still flexible and could tolerate imposed deformations without significant fracture.

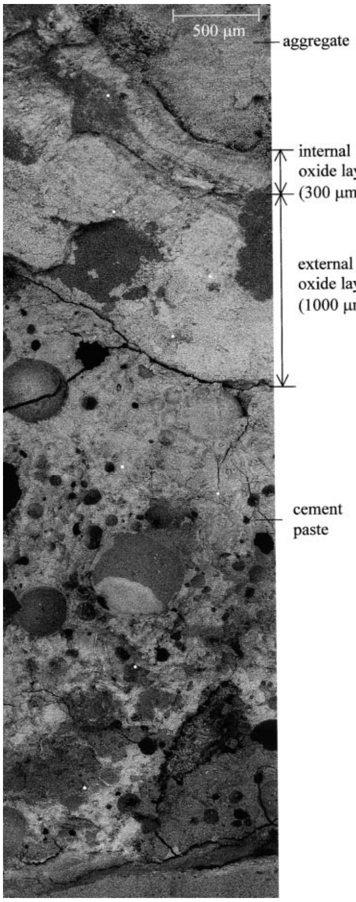

Fig. 3. Reproduction of the cement paste surface using backscattered electron images along line A shown in Fig. 2b. The white dots show the locations of the EDX element point analyses on this surface.

2.4. Energy dispersive spectroscopy analysis

The ESEM was fitted with an energy dispersive X-ray (EDX) spectrometer. X-ray point analyses were made in one specimen only in the region of the aggregate/cement paste interface to investigate the presence of various elements. The point analyses were carried out using an accelerating voltage of 20 keV at a magnification of 500 × . The elements identified are presented as summarized in Table 1.

The results show that in both the internal and external oxide layers, some spots can be identified, where there is predominantly calcium rather than iron. It is more likely that the calcium comes from the $Ca(OH)_2$ crystals that accumulate at the interface shortly after mixing of the concrete. No specific trend was observed concerning the distribution of chlorine (chloride ion) in the oxide layer or in the cement paste.

3. Discussion

The mechanism of formation of the ITZ appears to be related to the transportation of the more mobile ions during the hydration of cement. Maso [11] has proposed that the mechanism for the formation of the transition zone is the differential ionic concentration between the zone and the rest of the paste. Within the first few hours after mixing, a water-rich layer forms around the aggregate particles. The pore solution changes, ultimately becoming a solution of alkali hydroxides. The low ionic concentration at the zone, compared to that of the rest of the paste, results in ionic transportation by diffusion according to Fick's law. The higher diffusivity in the ITZ could explain the preferential accumulation of iron ions at the aggregate/cement paste

Table 1
Summarized results of EDX point analysis of elements (% atom) along the lines shown in Fig. 2b

Elements	O	Ca	Fe	Cl	Na	Mg	Si	K	Al	S
Internal oxide layer	56	8	32	1.5	0.9	1.2	0.2	0.2	0.1	0.3
	64	10	23	1.3	0.4	1.1	0.3	0.2	0	0.3
	56	7	22	1.3	0.9	11.2	0.8	0.2	0.6	0.2
	65	31	3	0.1	0.4	0.4	0.1	0.1	0.1	0.2
External oxide layer	58	4	35	0.8	0.8	0.2	0.2	0	0.2	0.1
	38	5	54	1.0	1.2	0.2	0.4	0.4	0.2	0.2
	65	7	25	0.3	1.2	0.1	0.2	0.2	0.1	0.2
	65	5	25	2.1	1.5	0.8	0.5	0.2	0.6	0.3
	48	9	37	1.0	1.2	0.8	1.1	0.3	0.7	0.6
	62	3	32	0.4	1.2	0.5	0.4	0.2	0.4	0.2
	66	3	26	0.8	2.6	0.2	0.5	0.5	0.2	0.2
	68	26	5	0.2	0	0.2	0	0.3	0	0.1
	52	44	3	0.1	0	0.1	0.3	0.2	0.1	0.2
	72	23	4	0.2	0.3	0.2	0.5	0.1	0.2	0.2
Cement paste	37	19	39	2.5	0.7	0.1	0.7	0.4	0.1	0.4
	41	4	45	1.6	0.6	0.2	6.4	0.4	0.5	0.3
	58	11	26	1.2	0	0.4	2.5	0.3	0.5	0.4
	70	5	19	1.8	0.8	0.8	2.6	0.2	0.5	0.4
	56	14	26	0.5	0	0	3.7	0	0	0
	40	12	32	1.6	1.4	0.9	7.7	1.8	1.6	1.0
	71	5	20	1.3	0.4	0.4	1.0	0.2	0.4	0.3
	68	9	20	1.5	0.3	0	0.7	0.3	0.2	0.4
	59	13	22	1.5	1.0	0.3	1.6	0.4	0	0.6
	58	9	25	2.1	1.3	0.7	2.6	0.4	0.6	0.4
	69	6	17	1.2	0.8	0.5	4.6	0.3	0.9	0.4
	69	9	15	1.2	1.4	0.6	2.5	0.2	0.4	0.4
	69	7	16	1.3	1.2	0.8	3.7	0.2	0.5	0.4
	66	6	19	1.4	1.5	0.9	3.7	0.2	0.6	0.3
	58	13	20	1.5	1.0	0.7	4.8	0.3	0.8	0.6
	66	22	1	0.4	0.8	0.4	5.6	0.6	1.7	0.7
	68	13	1	2.1	0.8	4.1	9.0	0.3	0.9	0.6
	88	10	0	0.4	0	0	1.6	0	0	0

The measurements were carried out using an accelerating voltage of 20 keV at a magnification of 500 ×.

interface rather than in the rest of the cement paste. Considering that the concrete mixtures contained a high concentration of chloride ion, it should be expected that corrosion of iron would start shortly after casting the specimens, when the chloride ions first come in contact with the surface of the steel bar.

However, the mechanism described above cannot explain the formation of different iron oxides in the inner and outer oxide layers. It is known that corrosion of iron results in the release of ferrous and to a lesser extent of ferric ions into the solution. Depending on the particular composition of the solutions (pH, presence of specific anions) and on the redox conditions of the environment, ferrous and ferric ions can then take place in a large number of reaction sequences, resulting to the formation of different solid oxide phases.

It has been reported that a thin duplex layer composed of $Ca(OH)_2$ forms on the aggregate surface, irrespective of the rock type, as irregular but conspicuous coatings having a thickness of about 2–3 μm [12,13]. This layer is followed by a contiguous calcium silicate hydrate (CSH). The amount of $Ca(OH)_2$ within the first 20 μm from the aggregate surface has been reported to be significantly higher than that in the bulk cement paste [14,15]. A saturated $Ca(OH)_2$ solution has a pH value of 12.6 at 25°C.

Several investigations on the composition of pore solutions in cement-based materials have shown that the pore liquid is a mixed solution of sodium hydroxide and potassium hydroxide, with a pH in the range 13.2–13.5 [16,17]. The chemical composition of the cement paste and its properties becomes more complicated in the presence of other ions. It has been reported in the past that chloride ion in the cement paste increases the size and changes the orientation of the $Ca(OH)_2$ crystals in the ITZ, and reduces the amount of $Ca(OH)_2$ in the bulk cement paste, but does not seem to affect the amount of $Ca(OH)_2$ in the ITZ [14].

In considering the mechanism, it is reasonable to assume that the initial corrosion product that is formed away from the steel bar surface is ferrous hydroxide, $Fe(OH)_2$. This compound reacts with water in a reaction known as the Schikorr reaction, in which ferrous ions are oxidized by water yielding magnetite and hydrogen [18]. The reaction predicts that the ferrous ions will form magnetite (Fe_3O_4) as it is described by Eq. (1), or will convert into ferric ions and form hematite (α-Fe_2O_3) as shown by Eq. (2).

$$3Fe(OH)_2 \rightarrow Fe_3O_4 + 2H_2O + H_2 \qquad (1)$$

$$Fe^{2+} \xrightarrow{O_2} Fe^{3+} \xrightarrow{H_2O} \alpha - Fe_2O_3 \qquad (2)$$

Accordingly, a viable explanation of the bilayer oxide structure observed at the aggregate/paste interface is the transport of Fe^{2+} from the corroding steel bar to the ITZ where, because of the high pH induced by $Ca(OH)_2$ saturation, hydrolysis occurs, resulting in the precipitation of $Fe(OH)_2$. This compound subsequently reacts to form magnetite via Eq. (1) at the immediate aggregate/cement paste interface of locally lower pH (12.6 compared to 13.2 in the cement paste). However, much of the Fe^{2+} is oxidized to Fe^{3+} by ambient oxygen, which subsequently hydrolyzes to $Fe(OH)_3$ and ultimately to α-Fe_2O_3 (hematite). This reaction occurs as the Fe^{2+} diffuses out of the $Fe(OH)_2$ (and hence, the Fe_3O_4) formation zone and consequently results in the outer Fe(III) oxide layer. In addition, ferric ion may be further transported into pores in the surrounding cement paste, where additional oxide precipitation occurs.

This mechanism could explain as well the formation of different types of iron oxides in the same order, i.e. magnetite at the immediate interface and hematite close to the paste, around a steel bar corroding in concrete that has been reported elsewhere [5].

4. Conclusions

From this study, the following conclusions can be drawn.

- Iron ions set free from a corroding steel bar embedded in concrete can accumulate around aggregates in close proximity to the steel bar. The higher diffusivity in the ITZ results in preferential accumulation of iron ions at the interface rather than in the rest of the cement paste.
- The iron oxides forming at the ITZ can have a high thickness of 1.5 mm. Local differences of the pore solution of the ITZ can account for formation of different types of iron oxides in the inner oxide layer (at the aggregate surface) and in the outer oxide layer (in contact with the cement paste).
- The type of oxide formed in either layer is postulated to depend on a competition between the Schikorr reaction resulting in magnetite in the inner layer and Fe^{2+} diffusion followed by oxidation and hydrolysis to form hematite (α-Fe_2O_3) in the outer layer.

Acknowledgments

The authors wish to thank Prof. F.H. Wittmann for his comments and suggestions. The first author is grateful to the Gerondelis Foundation for its financial support to carry out the research in the study.

References

[1] P.J.M. Monteiro, J.C. Maso, J.P. Ollivier, The aggregate–mortar interface, Cem Concr Res 15 (1985) 953–958.
[2] S. Diamond, J. Huang, The interfacial transition zone: Reality or myth? in: A. Katz, A. Bentur, M. Alexander, G. Arliguie (Eds.), The Interfacial Transition Zone in Cementitious Composites, E&FN Spon, London, 1998, pp. 3–39.
[3] C.L. Page, Mechanism of corrosion protection in reinforced concrete marine structures, Nature 258 (1975) 514–515.
[4] P.J.M. Monteiro, O.E. Gjorv, P.K. Mehta, Microstructure of the steel–cement paste interface in the presence of chloride, Cem Concr Res 15 (1985) 781–784.
[5] J.L. Gallias, Microstructure of the interfacial transition zone around corroded reinforcement, in: A. Katz, A. Bentur, M. Alexander, G. Arliguie (Eds.), The Interfacial Transition Zone in Cementitious Composites, E&FN Spon, London, 1998, pp. 171–178.
[6] D. Breton, A. Carles-Gibergues, G. Ballivy, J. Grandet, Contribution to the formation mechanism of the transition zone between rock–cement paste, Cem Concr Res 23 (1993) 335–346.
[7] J.P. Ollivier, M. Massat, The effect of the transition zone on transfer properties of concrete, in: J.C. Maso (Ed.), Interfacial Transition Zone in Concrete, RILEM Rep 11, E&FN Spon, London, 1996, pp. 117–131.
[8] D. Bonen, Features of the interfacial transition zone and its role in secondary mineralization, in: A. Katz, A. Bentur, M. Alexander, G. Arliguie (Eds.), The Interfacial Transition Zone in Cementitious Composites, E&FN Spon, London, 1998, pp. 224–233.
[9] F.P. Glasser, K.K. Sagoe-Crentsil, Steel in concrete: Part II. Electron microscopy analysis, Mag Concr Res 41 (1989) 213–220.
[10] K. Aligizaki, Modeling of concrete cracking due to corrosion of embedded reinforcement, PhD Thesis, The Pennsylvania State University, May 1999.
[11] J.-C. Maso, The bond between aggregates and hydrated cement pastes, in: 7th International Congress on the Chemistry of Cement, Paris, France Vol. 1, (1980) VII-1/3–VII-1/15.
[12] B.W. Barnes, S. Diamond, W.L. Dolch, Micromorphology of the interfacial zone around aggregate in Portland cement mortar, J Am Ceram Soc 62 (1979) 21–24.
[13] D. Bonen, Calcium hydroxide deposition in the near interfacial zone in plain concrete, J Am Ceram Soc 77 (1994) 193–196.
[14] M. Saito, M. Kawamura, Effects of sodium chloride on the hydration products in the interfacial zone between cement paste and alkali-reactive aggregate, in: J.C. Maso (Ed.), Interfaces in Cementitious Composites, E&FN Spon, London, 1993, pp. 33–41.
[15] D. Breton, G. Ballivy, Correlation between the transport properties of the transition zone and its mineral composition and microstructure, in: H. Jennings, J. Kropp, K. Scrivener (Eds.), The Modeling of Microstructure and Its Potential for Studying Transport Properties and Durability, NATO ASI Series Vol. 304, Kluwer Academic Publishing, Dordrecht, 1996, pp. 361–372.
[16] C.L. Page, K.W.J. Treadaway, Aspects of the electrochemistry of steel in concrete, Nature 297 (1982) 109–115.
[17] S. Diamond, Effects of two Danish flyashes on alkali contents of pore solutions of cement–flyash pastes, Cem Concr Res 11 (1981) 383–394.
[18] G. Schikorr, Über die Reaktionen zwischen Eisen, seinen Hydroxyden und Wasser, Z Elektrochem 35 (1929) 65–70.